

# ACCURATE REGISTRATION OF DYNAMIC CONTRAST-ENHANCED BREAST MR IMAGES WITH ROBUST ESTIMATION AND LINEAR PROGRAMMING

Yuanjie Zheng<sup>1</sup> and Andrew D. A. Maidment<sup>2</sup> and James C. Gee<sup>1</sup>

<sup>1</sup>PICSL, Department of Radiology, University of Pennsylvania, Philadelphia, PA, USA

<sup>2</sup>Radiology Department, Hospital of the University of Pennsylvania, Philadelphia, PA, USA

## ABSTRACT

Accurate registration of the dynamic contrast-enhanced (DCE) MR breast images is a well-known difficult problem. It is because the breast motion is non-rigid and the intensity variations of tumor between pre-contrast and post-contrast images can cause the unexpected tumor shrinking/expanding effect in the registration process. To obtain accurate registration, we propose two techniques: a novel image similarity measure based on the robust estimation and a new global optimization technique by reformulating the registration problem as solving a linear programming. The novel similarity measure can help to handle the shrinking/expanding problem while the global optimization technique offers more accurate estimation of the breast motion.

## 1. INTRODUCTION

Image registration is a vital process in the dynamic contrast-enhanced (DCE) magnetic resonance (MR) imaging based breast tumor diagnosis. DCE-MR imaging process generally involves multi-times of imaging before and after the administration of a contrast agent, yielding the pre-contrast image and a series of post-contrast images. In DCE-MR images, tumor region can have various contrast enhancement pattern due to the agent, leading to significant temporal intensity changes. The analysis on the enhancement curve which describes the temporal changes of intensity of a single pixel or a local region constructs the fundamentals of the diagnosis with DCE-MR images. Image registration, which can provide accurate spatial alignment of DCE-MR images taken at different time, plays a critical role in offering accurate enhancement curves.

However, accurate registration of DCE-MR images is plagued mainly with two challenges: the temporal changes of image intensity, and the non-rigidity of the breast motion in the imaging process. The intensity changes can produce volume shrinking/expanding effect of tumor in the process of registration [1]. This unexpected volume variation is not consistent with the assumption that the soft tissue is incompressible in the imaging process because of the small deformations involved and the short time imaging durations. As the other challenge, the nonrigid motion of breast makes the registra-

tion more complicated in both modeling and estimating the deformations.

To address the above challenges, different mechanisms have been proposed. To avoid or alleviate the tumor shrinking/expanding problem caused by the temporal intensity changes, there are many methods using some special regularization terms on the deformation field [1, 2, 3] or accounting for the enhancement effect [5]. However, most of them need some extra processing like the identification of tumor [1, 2], or the estimation of enhancement curve [5], etc. The registration accuracies significantly rely on the results of the extra processing. In these previous work, the free-form deformation (FFD) model based B-spline [6] was probably the most widely used model for its easiness to use and efficiency. However, most optimization strategies are gradient decent based, with which only a local minimum can be guaranteed and the results are highly dependent on the initialization. Some other techniques like the simulated annealing can produce a global optimization but require a lot of time.

In this paper, we propose two novel techniques for accurate registration of DCE-MR breast images, which can efficiently handle the challenges mentioned above. We first introduce a new image similarity measure in registration based on the robust estimation function [7]. It can account for the temporal intensity changes, resulting in the alleviation of the tumor shrinking/expanding problem without any extra processing. We then formulate the optimization of the FFD B-spline deformation model in image registration as recursively solving a linear programming problem [8]. Our algorithm can obtain a more optimal optimization compared with previous work. Comprehensive experiments demonstrate the effectiveness and high accuracy of our approach.

## 2. METHODS

Given two images  $\mathcal{I}$  and  $\mathcal{J}$ , our goal is to find an optimal geometrical transformation  $\mathcal{T}$  from  $\mathcal{I}$  to  $\mathcal{J}$  and constructs the mapping of the voxels (volume pixels) in  $\mathcal{I}$  to  $\mathcal{J}$ . The optimal  $\mathcal{T}$  is found by maximizing a similarity measure between the overlapping regions of the transformed image  $\mathcal{T}(\mathcal{I})$  of  $\mathcal{I}$  and  $\mathcal{J}$ . We next explain in detail three critical elements in our registration algorithm: the representation of  $\mathcal{T}$  in sec 2.1, the

energy function to be minimized in order to estimate  $\mathcal{T}$  in sec 2.2, and the optimization strategy in sec 2.3.

There are basically two significant contributions in our approach. First, we propose a new similarity measure based on the robust estimation function [7]. It can account for the temporal intensity changes in the DCE-MR data without any extra processing, as explained in sec 2.2. Second, we introduce a new optimization strategy accomplished by recursively solving a linear programming [8] problem, for which a global optimization can be obtained in each iteration without any initialization, as explained in sec 2.3.

## 2.1. Transformation Model

The transformation  $\mathcal{T}$  in our registration algorithm is composed of a global transformation  $\mathcal{T}_G$  and a local transformation  $\mathcal{T}_L$ . For an image point  $\mathbf{x} = (x, y, z)^T$  in the 3D image  $\mathcal{I}$ , where  $x, y$  and  $z$  are the coordinates, we then have

$$\mathcal{T}(\mathbf{x}) = \mathcal{T}_G(\mathbf{x}) + \mathcal{T}_L(\mathbf{x}). \quad (1)$$

Global transformation  $\mathcal{T}_G$  is set as the affine transformation, and the parameters are estimated by the iterative multi-resolution search strategy [6] with the Sum of Squared Difference (SSD) similarity measure.

Local transformation  $\mathcal{T}_L$  is given by the (FFD) model based cubic B-splines in [6]. However, to estimate it, we will use a more robust similarity measure (in sec 2.2) and a more efficient optimization strategy (in sec 2.3).

The basic idea of the FFD based B-splines is to deform the image through manipulating an underlying lattice of uniformly spaced control points (CPs) (denoted by set  $\Psi$ ). The transformation  $\mathcal{T}_L(\mathbf{x})$  is simply computed by interpolating the displacements of CPs in a CP subset  $\Psi_{\mathbf{x}} \subset \Psi$  denoting the closest  $4 \times 4 \times 4$  CPs surrounding  $\mathbf{x}$ . The 3D splines based on  $\Psi_{\mathbf{x}}$  can be treated as the tensor product of the independent 1D spline functions [3] on the three axes.

To define the 1D spline function, we take the  $x$ -axis for an example. Apparently, there are totally four different  $x$ -axis indices for the CPs in  $\Psi_{\mathbf{x}}$  and hence we can use four 1D spline functions for the interpolations, considering the CPs in  $\Psi_{\mathbf{x}}$  are distributed on a lattice. Let  $u$  denote the relative position of  $\mathbf{x}$  to the CPs with the second-low coordinate value on the  $x$ -axis. The four 1D basis function of the B-spline can be denoted by  $B_0(u), B_1(u), B_2(u),$  and  $B_3(u)$ , representing the interpolation coefficients with respect to the CPs in  $\Psi_{\mathbf{x}}$  from left to right, respectively. The expressions of the 1D spline functions are referred to [6]. For other two axes, similar to  $u$ , we use  $v$  and  $w$  to represent the relative positions of  $\mathbf{x}$  to the CPs with the second-low coordinate value on the  $y$ -axis and  $z$  axis, respectively. The corresponding 1D spline functions  $B_0(v), \dots, B_3(v)$  and  $B_0(w), \dots, B_3(w)$  have the same forms with  $B_0(u), \dots, B_3(u)$ , respectively.

Let  $(l_0, m_0, n_0)$  denote the the CPs in  $\Psi_{\mathbf{x}}$  with the lowest

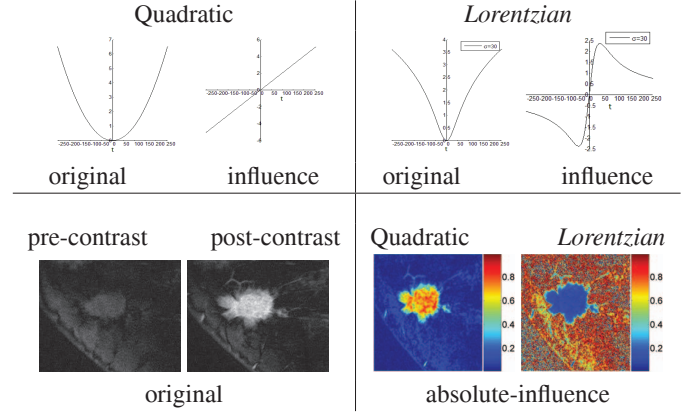


**Fig. 1.** Upper: quadratic and *Lorentzian* estimation functions and their influence functions. Lower: Original beast MR images (left) and the corresponding color-coded pixel-wise absolute-influence function value. The *Lorentzian* de-emphasizes tumor pixels more while the quadratic emphasize them more.

coordinate value on all three directions, we have

$$\mathcal{T}_L(\mathbf{x}) = \sum_{l=0}^3 \sum_{m=0}^3 \sum_{n=0}^3 B_l(u)B_m(v)B_n(w)\phi_{l_0+l, m_0+m, n_0+n} \quad (2)$$

where  $\phi$  denotes the displacement of a CP.

## 2.2. Energy Function

The estimation of the local transformation expressed in Eq. (2) can be formulated as the minimization of an energy function. Our energy function has two terms as in many other methods [2, 6, 3, 9]: a data term  $E_d$  to characterize the similarity between the transformed image and the target image, driving force behind the registration process and aims to minimize the matching cost between the two images; and a smoothness term  $E_s$  to regularize the transformation field, discouraging certain improbable or impossible transformation. It is written as

$$E = E_d + \lambda E_s = \sum_{p \in \mathcal{I}'} C(\mathcal{I}'(p) - \mathcal{J}(p)) + \lambda \sum_{p \in \mathcal{I}'} \sum_{p' \in \mathcal{N}_p} \|\mathcal{T}_L(p) - \mathcal{T}_L(p')\|^2 \quad (3)$$

where  $\mathcal{I}' = \mathcal{T}_L(\mathcal{I})$ ,  $\mathcal{I}'(p)$  means the image value of  $p$  in  $\mathcal{I}'$ ,  $C$  models the matching cost,  $\mathcal{N}_p$  represents the neighboring voxels of  $p$ ,  $\|\cdot\|$  is the  $L_2$  norm,  $\lambda$  is an adjusting parameter (e.g. 0.01) balancing the two terms. Obviously, the unknowns in Eq. (3) are the  $\phi$  values for each CP in Eq. (2).

To specify the matching cost function  $C$  in Eq. (3), for the intra-modality registration (the topic of the paper), the SSD [9] measure is a sensible choice. However, due to the temporal intensity changes in DEC-MR data, the shrinking/expanding problem of tumor [1] can inevitably happen. One significant contribution of this paper is the introduction

of a new matching cost measure to solve this problem, by replacing the  $C$  function in Eq. (3) with any robust estimation function [7]. We choose the *Lorentzian* estimator:

$$\rho(t) = \log(1 + (t/\sigma)^2/2) \quad (4)$$

where  $\sigma$  is a scale parameter to control the function's shape.

Without sacrificing the simplicity, the incorporation of the *Lorentzian* function in Eq. (3) is extremely efficient in handling the temporal intensity changes. The problem of the SSD measure (and other previous measures) is that the outlying measurements corresponding to the temporal intensity changes in DCE-MR images are assigned a high "weight". The CPs' movements are driven more by the unreliable intensity differences, leading to the shrinking/expanding problem in registration. In contrast, the *Lorentzian* function is more forgiving about the outlying measurements, reducing the driving force from the temporal intensity changes. The differences between the *Lorentzian* and quadratic functions can be seen from their influence functions [7] which characterize the bias of a particular measurement on the solution, as shown in Fig. 1. Different from the increasing property in the influence function of the quadratic measure, the influence function of the *Lorentzian* is redescending for which the influence of outliers tends to zero.

To specify  $\sigma$  in Eq. (4), we denote all voxels' intensity differences in the first term of Eq. (3) with  $\mathcal{X}$ , then

$$\sigma = c_x \text{MED}(|\mathcal{X} - \text{MED}(\mathcal{X})|) \quad (5)$$

where MED refers to the median value, and  $c_x$  is a constant that depends on the statistical distribution of  $\mathcal{X}$ . We simply set  $c_x = 1.4826$  by assuming  $\mathcal{X}$  is normally distributed.

### 2.3. Optimization

We novelly propose to recursively solve a linear programming formulation [8] to minimize the energy function in Eq. (3). Each iteration can produce a global optimization, resulting in a more optimal solution of the the registration.

We reformulate the two terms in Eq. (3) to facilitates the analysis. For the data term  $E_d$ , we approximate its minimization by recursively minimizing the sum of the matching costs each of which is caused independently by one CP's displacement. The displacement of any CP  $(i, j, k) \in \Psi$  only influences the motions of voxels in a subregion, denoted by  $\Upsilon_{(i,j,k)}$ , around it but not at all for other voxels [6]. The sum of matching costs of voxels in  $\Upsilon_{(i,j,k)}$  is denoted by  $C^{(i,j,k)}$ . The minimization of  $E_d$  in Eq. (3) can then be approximated by recursively minimizing the sum of  $\{C^{(i,j,k)}, (i, j, k) \in \Psi\}$ . Apparently, this strategy has already been implicitly used in the gradient decent based optimization methods [6, 3]. For the smoothness term  $E_s$  of Eq. (3), from Eq. (2), it is easy to see that  $\mathcal{T}_{\mathcal{L}}(p)$  and  $\mathcal{T}_{\mathcal{L}}(p')$  can both be written as a linear combination of  $\{\phi_{(i,j,k)}, (i, j, k) \in \Psi\}$ , and the same to  $\mathcal{T}_{\mathcal{L}}(p) - \mathcal{T}_{\mathcal{L}}(p')$ . Eq. (3) then becomes

$$E = \sum_{(i,j,k) \in \Psi} C^{(i,j,k)} + \lambda \sum_{p \in \mathcal{I}'} \sum_{p' \in \mathcal{N}_p} \left\| \sum_{(i,j,k) \in \Psi} \omega_{pp'}^{(i,j,k)} \phi_{(i,j,k)} \right\|^2 \quad (6)$$

where  $\omega_{pp'}^{(i,j,k)}$  represents the combination coefficient.

The energy function in Eq. (6) is nonlinear and usually highly non-convex, making it difficult to minimize without a good initialization. We construct the convex approximation for the individual matching cost surface of each CP, thus making the energy function convex. As a result, we can approximate the minimization of the energy function by recursively solving a linear programming problem [8], for which a global optimization can be obtained in each iteration. Specifically, for each CP  $(i, j, k)$  in  $\mathcal{I}'$ , we treat the displacements corresponding to the points comprising the facets of the lower convex hull of its matching cost surface as the basis displacements, denoted by  $\mathcal{B}_{\phi}^{(i,j,k)}$ , and then we can rewrite  $\phi_{i,j,k}$  as a linear combination of  $\phi_b$  in  $\mathcal{B}_{\phi}^{(i,j,k)}$ , i.e.

$$\phi_{i,j,k} = \sum_{\phi_b \in \mathcal{B}_{\phi}^{(i,j,k)}} \epsilon_{\phi_b}^{(i,j,k)} \phi_b \quad \text{with the constraints} \quad (7)$$

$$\epsilon_{\phi_b}^{(i,j,k)} \geq 0 \quad \text{and} \quad \sum_{\phi_b \in \mathcal{B}_{\phi}^{(i,j,k)}} \epsilon_{\phi_b}^{(i,j,k)} = 1.$$

$C^{(i,j,k)}$  in Eq. (6) can also be represented as a linear combination of the costs with  $\phi_b$ :  $C^{\phi_b}$ . Therefore, the minimization of Eq. (6) is formulated as

$$\arg \min \left\{ \sum_{(i,j,k) \in \Psi} \sum_{\phi_b \in \mathcal{B}_{\phi}^{(i,j,k)}} \epsilon_{\phi_b}^{(i,j,k)} C^{\phi_b} + \lambda \sum_{p \in \mathcal{I}'} \sum_{p' \in \mathcal{N}_p} \left\| \sum_{(i,j,k) \in \Psi} \omega_{pp'}^{(i,j,k)} \sum_{\phi_b \in \mathcal{B}_{\phi}^{(i,j,k)}} \epsilon_{\phi_b}^{(i,j,k)} \phi_b \right\|^2 \right\}. \quad (8)$$

The optimization in Eq. (8) with the constraints in Eq. (7) is a linear programming problem [8]. Different methods can be used to efficiently solve it. We chose the barrier method [8] due to its high efficiency. In [10], integer programming is used to solve a similar registration problem. However, in that work, CP displacement takes value from quantized labels. As shown by that paper, the number of labels influences greatly the registration accuracy and is impossibly set to infinity. In contrast, our method is free from this limitation and determines CP displacement as a continuous value.

## 3. RESULTS

The DCE-MR scans were acquired from 18 patients. Five post-contrast scans were obtained after the injection of the agent. The resolution is  $0.70 \times 0.70 \times 3.75$  mm<sup>3</sup>. In our registration, we set the CPs' spacing as 13mm.

To evaluate our new image similarity measure in sec 2.2 in handling the expanding/shrinking problem, we performed the registration with the optimization in sec 2.3 to map the post-contrast images on the pre-contrast images. The shrinking/expanding effects were measured by the absolute percentage of the tumor volume changing relative to the original volume. We selected 48 pairs of pre-contrast and post-contrast images, such that a wide range of tumor shapes, sizes, and temporal intensity changes can be covered. The tumors were

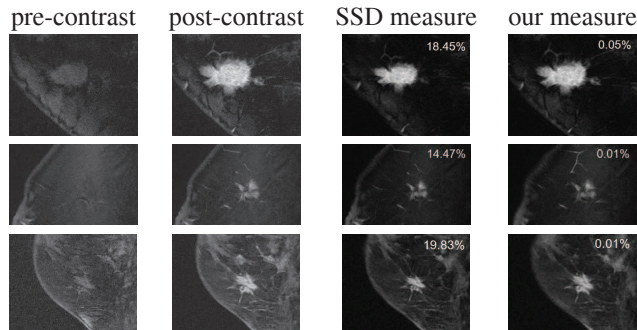


**Fig. 2.** Examples of registration results on DCE-MR breast images with the SSD measure and our new similarity measure. The numbers of the absolute tumor shrinking/expanding percentage are labeled on the corresponding image.

manually segmented by an experienced rater. From the experiments, we found that the mean and standard deviation (STD) of the percentages with SSD are 19.87% and 13.45%, respectively, and in contrast, the mean and STD with our new similarity measure are 0.04% and 0.01%, respectively. Our new similarity measure is extremely efficient in handling the shrinking/expanding problem. Some example images and the corresponding results are shown in Fig. 2.

To show the efficiency of our new optimization technique in sec 2.3, we compared the registration accuracies with the gradient decent method in [6]. We chose 16 pairs of pre-contrast and post-contrast images for which the patient's motion is negligible through visually checking the intensity differences between them by an experienced rater. We then added some artificial deformations on the post-contrast images, constructed using the model in sec 2.1 with CPs' spacing 55mm. We added a motion on each CP with a random displacement between 0mm and 8mm and along a random direction in the 3D space. The registration accuracy was then assessed by computing the mean and STD of the absolute deformation errors of all voxels and over all image pairs. From the results, we found that the mean and STD of errors by the gradient decent method [6] are 8.7mm and 5.1mm, respectively, and in contrast, the values of our linear programming based optimization are 4.1mm and 3.2mm, respectively. It means that our optimization technique can obtain a more optimal solution.

Through the experiments, we found that the minimization of Eq. (8) needs to be minimized for four times at most to get an optimal solution.

#### 4. CONCLUSIONS AND FUTURE WORK

We propose to use the robust estimation functions to measure the image similarity in registration and show that it can efficiently handle the shrinking/expanding problem in tumor caused by the temporal intensity changes in DCE-MR breast images. We also reformulate the energy minimization in the

FFD B-spline based registration as recursively solving a linear programming problem, for which, a global optimization can be obtained in each iteration, and a more optimal solution can be finally acquired, compared with the widely used gradient decent based methods.

Our energy minimization strategy with linear programming can be easily adjusted to other transformation model like the thin-plate spline [11], etc. We will do experiments to show the improvement in breast tumor diagnosis through incorporating our registration approach.

#### 5. REFERENCES

- [1] C. Tanner, J. A. Schnabel, D. Chung, M. J. Clarkson, D. Rueckert, D. L. G. Hill, and D. J. Hawkes, "Volume and shape preservation of enhancing lesions when applying non-rigid registration to a time series of contrast enhancing MR breast images," in *MICCAI 2000*, 2000, pp. 327–337.
- [2] J. A. Little, D. L. G. Hill, and D. J. Hawkes, "Deformations incorporating rigid structures," *Computer Vision and Image Understanding*, vol. 66, pp. 223–232, 1997.
- [3] Torsten Rohlfing, Calvin R. Maurer, David A. Bluemke, and Michael A. Jacobs, "Volume-preserving nonrigid registration of MR breast images using free-form deformation with an incompressibility constraint," *IEEE Transactions on Medical Imaging*, vol. 22, pp. 730–741, 2003.
- [4] Dirk Loeckx, Frederik Maes and Dirk Vandermeulen, and Paul Suetens, "Nonrigid image registration using free-form deformations with a local rigidity constraint," in *MICCAI 2004*, 2004, vol. 3216, pp. 639–646.
- [5] Xiaohua Chen, Michael Brady, and Jonathan Lo, "Simultaneous segmentation and registration of contrast-enhanced breast MRI," in *IPMI 2005*, 2005, vol. 3565, pp. 126–137.
- [6] D. Rueckert, L. Sonoda, I. C. Hayes, D. L. G. Hill, M. O. Leach, and D. J. Hawkes, "Nonrigid registration using free-form deformations: Application to breast MR images," *IEEE Transactions on Medical Imaging*, vol. 18, pp. 712–721, 1999.
- [7] Frank R. Hampel, Elvezio M. Ronchetti, Peter J. Rousseeuw, and Werner A. Stahel, *Robust Statistics: The Approach Based on Influence Functions*, Wiley, New York, 1986.
- [8] Jiri Matousek and Bernd Gartner, *Understanding and Using Linear Programming*, Springer, 2007.
- [9] Jan Kybic and Michael Unser, "Fast parametric elastic image registration," *IEEE Transaction on Image Processing*, vol. 12, pp. 1427–1442, 2003.
- [10] Ben Glocker, Nikos Komodakis, Nikos Paragios, Georgios Tziritas, and Nassir Navab, "Inter and intra-modal deformable registration: Continuous deformations meet. efficient optimal linear programming," in *IPMI 2007*, 2007, pp. 408–420.
- [11] Yujun Guo, Radhika Sivaramakrishna, Cheng-Chang Lu, Jasjit S. Suri, and Swamy Laxminarayan, "Breast image registration techniques: a survey," *Medical and Biological Engineering and Computing*, vol. 44, pp. 15–16, 2006.